BNL-106300-2014-CP

Mini Compton Camera Based on an Array of Frisch-grid CdZnTe Detectors

Wonho Lee

A. Bolotnikov, G. Camarda, Y. Cui, R. Gul, A. Hossain, U. Roy, G. Yang, T. Lee, R. James

October 2014

Nonproliferation and National Security

Brookhaven National Laboratory

U.S. Department of Energy

Office of Nonproliferation and Verification Research and Development

Notice: This manuscript has been authored by employees of Brookhaven Science Associates, LLC under Contract No. DE-AC02-98CH10886 with the U.S. Department of Energy. The publisher by accepting the manuscript for publication acknowledges that the United States Government retains a non-exclusive, paid-up, irrevocable, world-wide license to publish or reproduce the published form of this manuscript, or allow others to do so, for United States Government purposes.

DISCLAIMER

This report was prepared as an account of work sponsored by an agency of the United States Government. Neither the United States Government nor any agency thereof, nor any of their employees, nor any of their contractors, subcontractors, or their employees, makes any warranty, express or implied, or assumes any legal liability or responsibility for the accuracy, completeness, or any third party's use or the results of such use of any information, apparatus, product, or process disclosed, or represents that its use would not infringe privately owned rights. Reference herein to any specific commercial product, process, or service by trade name, trademark, manufacturer, or otherwise, does not necessarily constitute or imply its endorsement, recommendation, or favoring by the United States Government or any agency thereof or its contractors or subcontractors. The views and opinions of authors expressed herein do not necessarily state or reflect those of the United States Government or any agency thereof.

Mini Compton Camera Based on an Array of Frisch-grid CdZnTe Detectors

Wonho Lee, Aleksey Bolotnikov, Taewoong Lee, Giuseppe Camarda, Yonggang Cui, Rubi Gul, Anwar Hossain, Roy Utpal, Ge Yang, and Ralph James

Abstract— **We constructed a mini Compton camera based on an array of CdZnTe detectors and assessed its spectral and imaging properties. The entire array consisted of 6×6 Frisch-grid CdZnTe detectors, each with a size of 6×6×15 mm^3. Since it is easier and more practical to grow small CdZnTe crystals rather than large monolithic ones, constructing a mosaic array of parallelepiped crystals can be an effective way to build a more efficient, large-volume detector. With the fully operational CdZnTe array, we measured the energy spectra for ^{133}Ba-, ^{137}Cs-, ^{60}Co-radiation sources; we also located these sources using a Compton imaging approach. Although the Compton camera was small enough to hand-carry, its intrinsic efficiency was several orders higher than those generated in previous research using spatially separated scintillator arrays, because our camera measured the interactions inside the CZT detector array, wherein the detector elements were positioned very close to each other.**

***Index Terms*—Compton Camera, Electronic Collimation, Frisch-Grid, CdZnTe**

I. Introduction

CdZnTe detectors have been used widely for measuring radiation energy because of their relatively high energy-resolution, high atomic number, and operability at room temperature [1]. However, due to the low mobility of holes in the material, and its non-uniformity, the usability of these crystals for planar gamma-detectors has been limited; hence, special designs were developed to ensure their suitability for field-portable gamma-ray spectrometers, such as the co-planar grid [2], the small pixel structure [3], [4], and the virtual Frisch-grid device [5], [6]. In current technology, the achievable size of a single crystal with high energy resolution is less than 6 cm^3 [7]. Hence, to construct a large-volume CdZnTe detector suitable for compact, inexpensive instruments, we developed an assembly of detector modules [8]-[11]. The merit of our method is that the size of the assembly is not limited by the size of a single crystal, and can be increased by merely adding elements. By assembling CdZnTe modules, we developed a mini-gamma camera without requiring any additional instruments. The CdZnTe modules measured and yielded information on the energy and position of sequential interactions inside the camera; we calculated the original position of the radiation sources by applying Compton imaging technology to the measured information. The feasibility of Compton imaging technology was proven several decades ago [12], [13], and it has been used for various detectors to reconstruct radiation sources. In the early stages of this research, most detector materials used for Compton imaging were gases or scintillators that could be present in a large volume and coupled with position-sensing devices [12]. With the development of semiconductor manufacturing, a Compton camera fabricated from semiconductors became available, as well as scintillators [14]-[18]. Compared to gases and scintillators, semiconductors show high energy-resolution so assuring fine angular resolution in the reconstructed Compton images. Semiconductors can also attain finer resolution in positioning than even their own pixel dimensions by using the timing information from, or the signal ratio of different electrodes, which improves the angular resolution of the reconstructed Compton image. There have been several research investigations on Compton cameras using one or more CdZnTe detectors, mostly with a single structure [14]-[16]. In this study, we discuss the performance of our Compton camera, consisting of a mosaic array of parallelepiped CdZnTe crystals; they have high potential to be built as a large-volume detector array, resulting in an increase in the efficiency of the detection, and the availability to apply mechanical collimation requiring a large sensing area with high energy- and position-resolution.

II. Materials and Methods

Fig. 1a shows a schematic diagram of a mosaic detector array for a mini Compton camera. Fig. 1b is a photograph of an individual element, whilst 1c shows the entire assembly. Figure 1d is the corresponding schematic diagram of a mini Compton camera. The assembly consisted of 6×6 CdZnTe detectors, each of which has a volume of 6×6×15 mm^3; the gap between them was 1.5 mm. Based on the

This work was supported by U.S. Department of Energy, Office of Defense Nuclear Nonproliferation Research & Development, DNN R&D, U.S. Defense Threat Reduction Agency (DTRA) and BNL's Technology Maturation Award. The manuscript has been authored by Brookhaven Science Associates, LLC under Contract No. DE-AC02-98CH1-886 with the U. S. Department of Energy.

This work was supported by the BK21plus (21A20132212094) funded by the Korean government (MEST).

W. Lee and T. Lee are with the Department of Bio-Convergence Engineering, Korea University, Seoul 136-701, Korea.

A. Bolotnikov, G. Camarda, Y. Cui, R. Gul, A. Hossain, R. Utpal, G. Yang, and Ralph James are with the Department of Nonproliferation and National Security, Brookhaven National Laboratory, Upton, NY 11973, USA

W. Lee is the corresponding author for this paper. (e-mail: wonhol@korea.ac.kr)

cathode-to-anode ratio and drift time, we corrected the information on the energy of the radiation interaction, so that we could calculate the depth-of-interaction position between the cathode and anode. We note that this was a prototype system, and its electronics could handle more than a tenfold increase in the number of detectors for further studies.

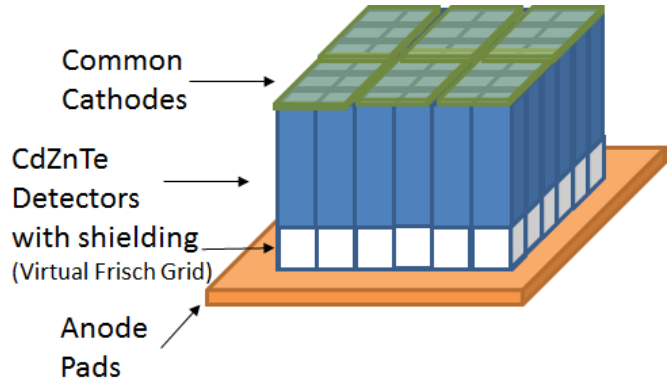

Fig. 1a. Schematic diagram of a mosaic array of parallelepiped CdZnTe crystals with electrodes.

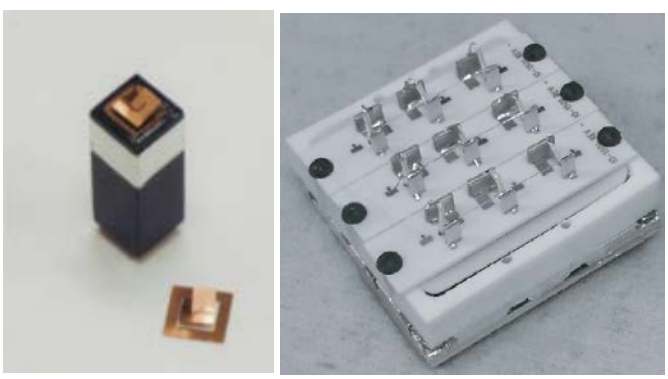

1 (b) 1(c)

Figs. 1b and 1c. Photograph of the detector array for a mini Compton camera, illustrating left, a single detector element, and right the assembled elements in it.

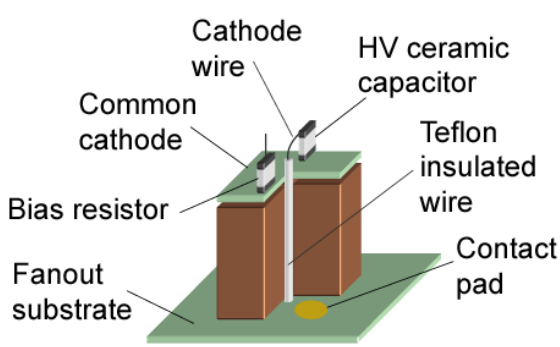

Fig. 1d. Schematic diagram of a detector assembly.

Since the position and energy information for each radiation interaction in the detectors are known, the location of the radiation source can be identified via Compton imaging technology. If the position and energy information of the source, 1st interaction and 2nd interaction, respectively, are (r_0, E_0), (r_1, E_1) and (r_2, E_2), the cosine values can be calculated based on this information as follows:

$$cos\theta_r = \frac{\bar{r}_1 \cdot \bar{r}_2}{|\bar{r}_1||\bar{r}_2|} \qquad \text{..... (1)}$$

$\bar{r}_1$: vector from r_0 to r_1

$\bar{r}_2$: vector from r_1 to r_2

$$cos\theta_E = 1 - m_0c^2\left(\frac{1}{E_2} - \frac{1}{E_1}\right) \qquad \text{..... (2)}$$

m_0c^2: the rest mass of the electron.

Equalizing the two cosine values, we then can calculate the source's position, r_0. Based on these above equations, we can draw a cone on the source planes for each interaction event. Fig. 2 illustrates how to draw a cone containing a source position. For interaction events, cosines of the angles (θ_{r0}, θ_{r1}, θ_{r2}, …) are calculated for each point (r_{00}, r_{01}, r_{02}, …) on a 1-D line, and, after comparing the cosines with $cos\theta_E$ calculated by (2), the pixel r_{00} whose cosine value of the angle (θ_{r0}) is closest to $cos\theta_E$, we chose as one of possible source positions. Likewise, if the 1-D line is expanded to the 2-D plane or the 3-D volume, other positions on the cone with a vertex r_1, an axis passing r_1 and r_2, and an angle θ_{r0} are selected as possible source positions. If we measure multiple events, the overlaps of the cones will indicate the source position.

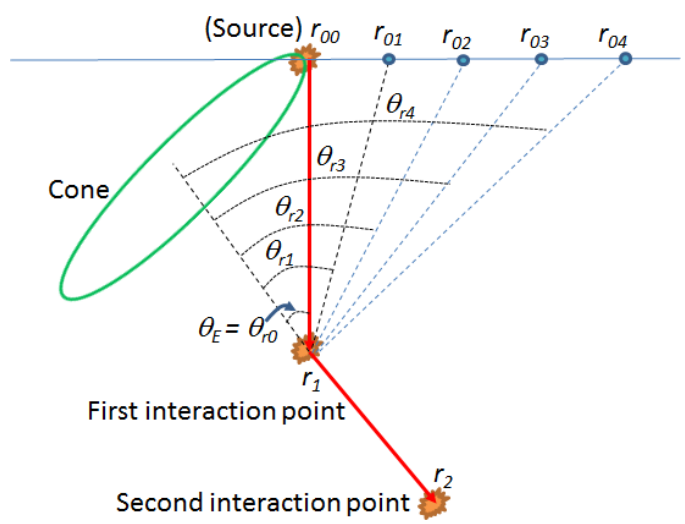

Fig. 2. Schematic diagram to identify a source's position and draw a cone.

Since the overlaps of the cones are a simple back-projection, including inherent angular broadening, additional image reconstruction is required to precisely locate the source's position. We used maximum likelihood expectation and maximization (MLEM) method for image reconstruction as shown in (3). This statistical reconstruction algorithm, including the Poisson distribution, is widely used in Compton imaging due to its effectiveness

for obtaining the reconstructed image with limited number of radiation measurements. [19], [20]

$$x_j^{n+1} = \frac{x_j^n}{\sum_i c_{ij}} \sum_i \frac{c_{ij} Y_i}{\sum_k c_{ik} x_k^n} \quad \text{..... (3)}$$

where x_j^{n+1} and x_j^n are (n+1)th and nth estimates of pixel values at the source plane where the initial values, x_j^0, all are positive. c_{ij} is the probability of ith detection event for an emitted photon at j^{th} source pixel. c_{ij} includes the angular probabilistic distribution of Compton scattering calculated by the Klein-Nishina formula, and the radiation attenuations in the detector divided by the square of the distances from the source plane to the 1st interaction point, and from that point to the 2nd interaction point. Y_i is the measured data for the detection event, *i*. For the regular MLEM method, the total number of possible combinations of the position- and energy- measurements was significantly larger than that of the detected photons needed to be considered, which requires a long calculation time and excessive data storage for a conventional computer. Therefore, instead we applied a list-mode MLEM, which considers each measurement unique (cf. $Y_i = 1$) [21].

The sequence of the interactions was determined by the energy of each one. According to Y. F. Du *et al.* [14] and W. Lee *et al.* [22], if the energy of the incident gamma ray was less than 400 keV, it is more probable that the first interaction deposits less energy than does the second interaction in two-events sequences, and vice versa. Therefore, for a 356-keV radiation, we chose the less energetic events as the first interaction, while the higher energy events were the first interactions for higher energy radiations (i.e., 356-, 662-, and 1275-keV).

The experimental setups were used to evaluate the performance of the mini Compton camera. First, point sources of 169.5-kBq ^{133}Ba (356 keV), 281.6-kBq ^{137}Cs (662 keV) and 7.8-kBq ^{60}Co (1173, 1332 keV) were located 14.5 cm from the top of the detector array. The measurement times for ^{133}Ba and ^{137}Cs were 2 hours, and that for ^{60}Co was 10 hours. In our second experiment, point sources of 169.5-kBq ^{133}Ba, 281.6-kBq ^{137}Cs, and 7.8-kBq Ci ^{60}Co were positioned at the vertexes of an equilateral triangle, and the radiations from all three were detected simultaneously. The plane with the multi-sources was placed 17 cm from the detector, and the distance between sources was 14.5 cm. The measurement time was 2 hours.

III. RESULTS

Fig. 3 lists shows the energy resolutions of the spectra for single events measured by each detector element. The resolutions were calculated at the full-width-half-maximum (FWHM) divided by the peak channel for 662-keV gamma rays. The energy resolution of the combined spectrum for all detector elements was 1.08 % (Fig. 4).

1.00	1.15	1.60	1.85	0.80	1.35
0.90	1.40	1.25	1.10	0.75	0.85
0.75	1.15	1.20	0.95	0.80	0.90
1.15	0.75	0.70	0.70	0.85	0.75
0.90	0.90	1.50	1.05	1.40	0.80
1.30	1.05	0.85	1.30	1.70	1.25

Fig. 3. Energy resolutions, in %, of the 6×6 CdZnTe detector for a ^{137}Cs source.

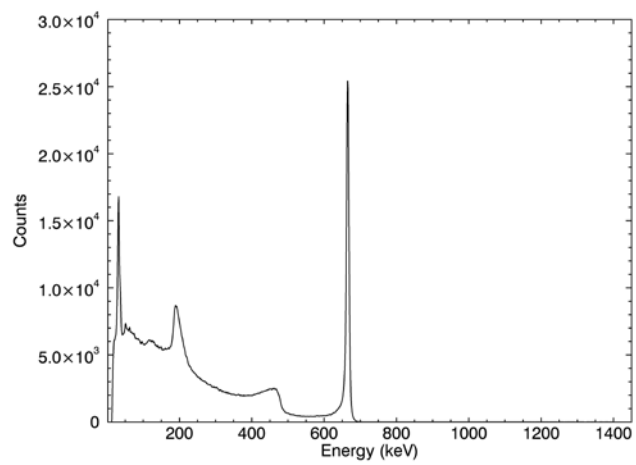

Fig. 4. Energy spectrum of all single events for a ^{137}Cs source.

Fig. 5 shows the spectra of the single- and coincident-events measured for ^{133}Ba, ^{137}Cs and ^{60}Co sources. The energy resolutions for ^{133}Ba (356 keV), ^{137}Cs (662 keV), and ^{60}Co (1173, 1332 keV), respectively were 1.96-, 1.36-, 1.19-, and 1.13-%. The energy resolution of the coincident events for a ^{137}Cs source was broader than that of the single events, because the energy resolution is inversely proportional to the deposited energy, and the individually deposited energies of a coincident event are lower than that of a single event. In addition, the electronic noise increases when each of the electronic signals induced by a sequential interaction is summed. The peak-to-total ratios of the spectra for coincident events were 2.7 times higher than that for single events, because most of the Compton continuum consists of single Compton scattering events, followed by the escape of the scattered gamma rays, whilst the photo-peak can be composed of coincident events, such as Compton scatterings followed by photoelectric events [23].

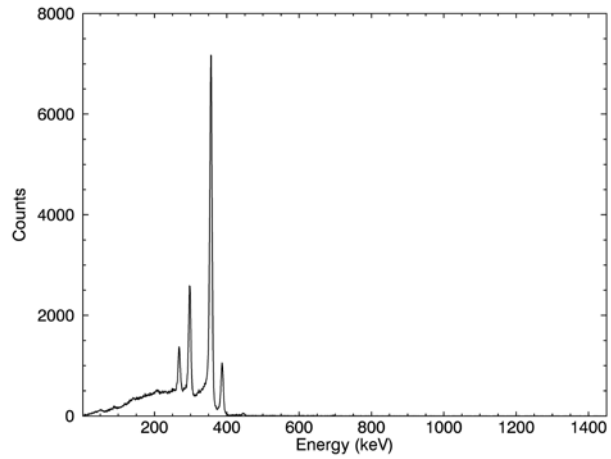

(a)

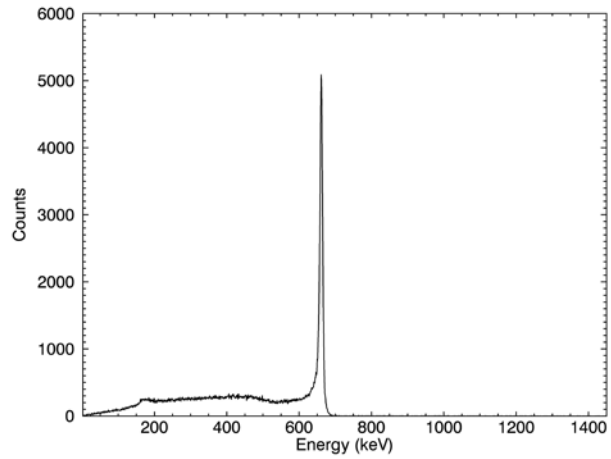

(b)

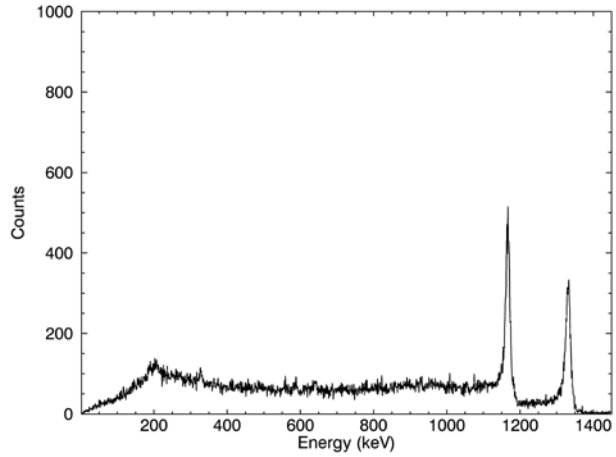

(c)

Fig. 5. Energy spectra of coincident events.

(a) ^{133}Ba (b) ^{137}Cs (c) ^{60}Co

Fig. 6 shows the angular resolution measurements (ARM) that illustrated the difference between the angles calculated based on the position and energy information (cf. (1) and (2)) when the location of the source was known as the center of the field-of-view (FOV). Since angular uncertainty is related to energy uncertainty and energy resolution is inversely proportional to a square root of the incident energy [24], the FWHM and FWTM (full width tenth maximum) of the ARM generally decreased proportionally with the increase of the incident radiation energy. The width of each back-projection cone for Compton imaging (cf. Fig. 2) was set based on that of the ARM.

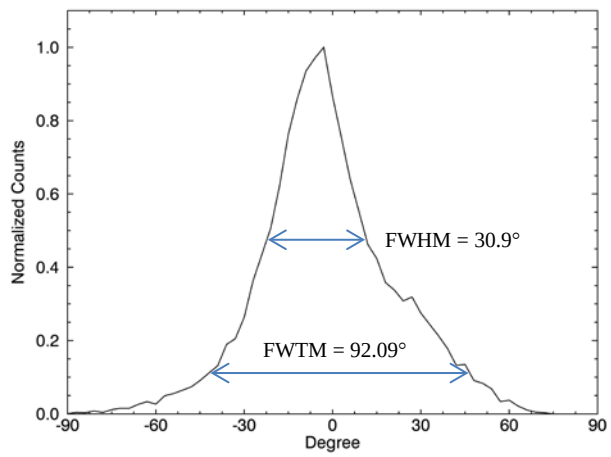

(a)

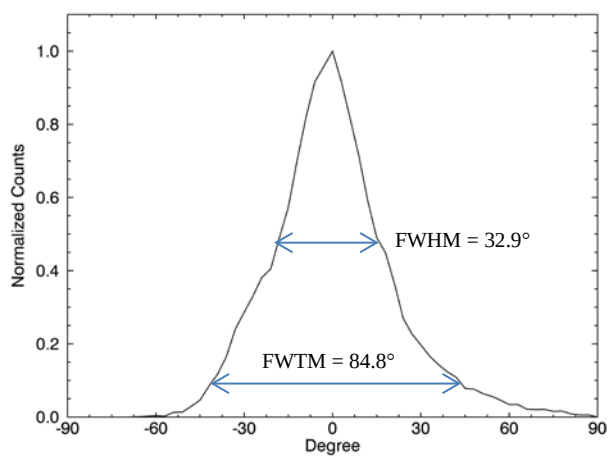

(b)

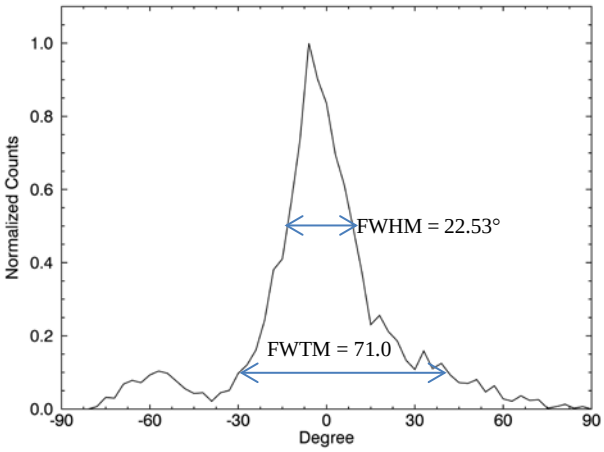

(c)

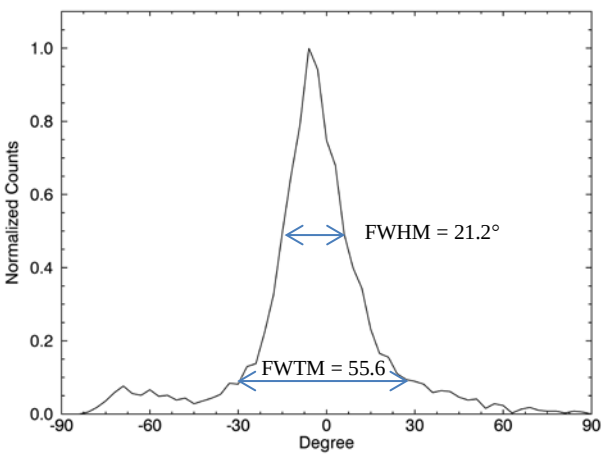

(d)

Fig. 5. ARM of reconstructed point sources.

(a) 356 keV (b) 662 keV (c) 1173 keV (d) 1332 keV

Fig. 6 showed the images of point isotopes reconstructed using the MLEM method. Only when the combined energy of two sequential events was in the range of the photo-peak region for each source, the events were selected for Compton reconstruction. As discussed in previous studies [25], [26], the reconstructed image was sharper and had more noise with higher iteration.

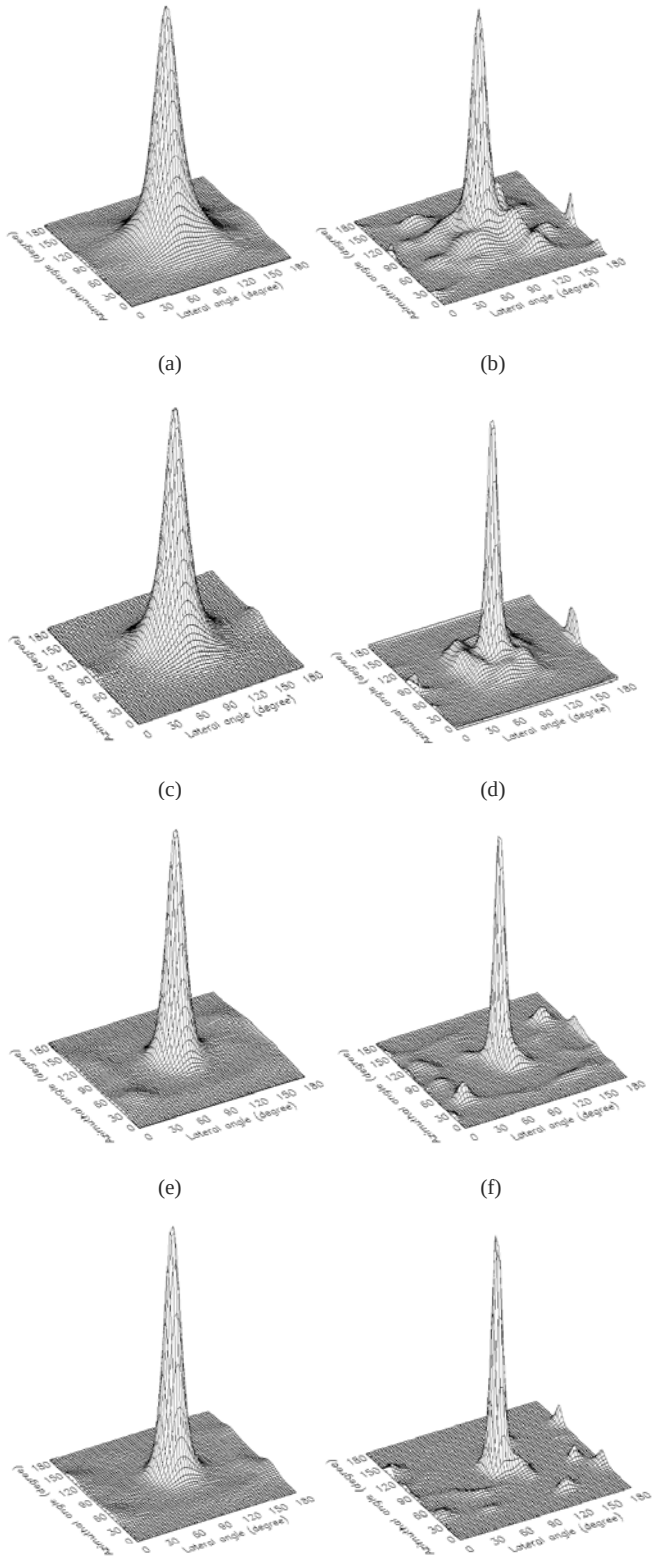

(a) (b) (c) (d) (e) (f) (g) (h)

Fig. 6. Reconstructed images of point sources with MLEM method

(a) 356 keV, 10th iteration (b) 356 keV, 100th iteration
(c) 662 keV, 10th iteration (d) 662 keV, 100th iteration
(e) 1173 keV, 10th iteration (f) 1173 keV, 100th iteration
(g) 1332 keV, 10th iteration (h) 1332 keV, 100th iteration

Table 1 shows the FWHMs, intrinsic efficiency, and absolute efficiency for each radiation source at 14.5 cm from the detector. The intrinsic imaging efficiency was the ratio of the number of effective events (a Compton scattering followed by a photoelectric effect) used for image reconstruction to the total number of gamma rays incident on the surface of the detector; the absolute efficiency was the ratio of the number of the same effective events to the total number of gamma rays emitted from the source.

TABLE I
MEASUREMENTS FOR VARIOUS RADIATION ENERGIES

Energy (keV)	FWHM (degree)		Efficiency	
	10th	100th	Intrinsic	Absolute (14.5 cm)
356	30.4	18.2	1.81×10^{-2}	8.73×10^{-5}
662	26.0	13.9	0.94×10^{-2}	4.53×10^{-5}
1173	20.3	12.6	0.50×10^{-2}	2.42×10^{-5}
1332	19.1	12.6	0.44×10^{-2}	2.12×10^{-5}

The efficiencies are inversely proportional to the energies of the sources, because the probability of both Compton scattering and photoelectric effect decreased with the rise in incident radiation energy. Compared to the results of previous research using two separated scintillator arrays, the detection efficiency of our camera was from two-to four-orders of magnitude higher, while the angular resolution was from two- to six-times broader than that of the previous cameras. By using an integrated detector array, we minimized the distance between voxels of our camera, and hence, the detection efficiency was significantly improved, but the geometrical uncertainty based on the ratio of the voxel size to the distance between voxels was increased.

TABLE II
COMPARISON OF THE PERFORMANCE FOR THREE DETECTION SYSTEMS

Performance	Compton cameras (662 keV, 50th iteration)		
	Integrated CZT detector (Frisch-grid)	Cubic CsI (Na) detector [25]	Paired $LaCl_3$(Ce) detector [26]
Angular resolution (°)	17.1	7.0	3.0
Intrinsic efficiency	0.94×10^{-2}	0.97×10^{-4}	2.27×10^{-6}

Fig. 7 shows the reconstructed images of multiple sources after the 50th iteration. Every source, which was measured simultaneously, clearly was identified in each of its own positions. In Fig. 7(a), multiple sources were reconstructed by summing the reconstructed image of each source after the peak-count normalization. The radius of each reconstructed source was inversely proportional to the energy of the gamma rays emitted from the source, which was consistent with the results in Table I.

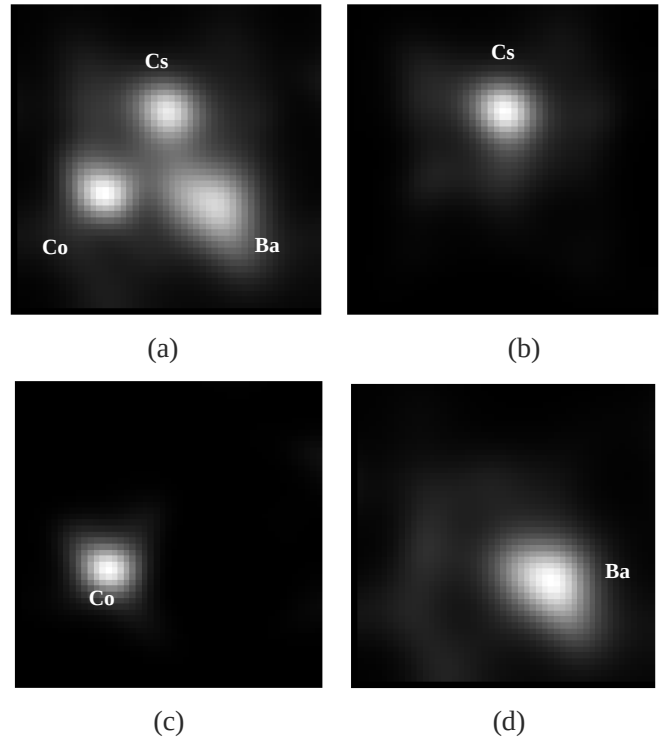

Fig. 7. Reconstructed images of multiple sources with MLEM method (50th iteration)
(a) All three sources (b) Cs (662 keV)
(c) Co (1173 and 1332 keV) (d) Ba (356 keV)

IV. CONCLUSIONS

By using an array of Frisch-ring CdZnTe detectors, we developed a mini Compton camera and compared its performance with those achieved by previous researchers based on separated scintillator arrays. The efficiency and angular resolution of our camera were experimentally measured for various gamma-ray sources (at energies of 356-, 662-, 1137- and 1332-keV). Our camera, consisting of an integrated array, has significantly higher detector efficiency and broader angular resolution than those made of separated scintillators. In further studies we will use a finer voxel or sub-voxel CdZnTe array to improve the camera's angular resolution.

REFERENCES

[1] T. E. Schlesinger and R. B. James, "Semiconductors and Semimetals," *in Semiconductors for Room Temperature Nuclear Detector Applications.* San Diego, CA: Academic, 1995, vol. 43. CD-ROM.

[2] P. N. Luke and E. E. Eissler, "Performance of CdZnTe Coplanar-Grid Gamma-Ray Detectors," *IEEE Trans. Nucl. Sci.*, vol. 43, No. 3, pp. 1481-1486, 1996.

[3] Z. He, W. Li, G. F. Knoll, D. K. Wehe, J. Berry, and C. M. Stahle, "3-D position sensitive CdZnTe gamma-ray spectrometers," *Nucl. Instr. Meth. A*, vol. 422, pp. 173-178, 1999.

[4] Feng Zhang, Zhong He, Dan Xu, Glenn F. Knoll, David K. Wehe, and James E. Berry "Improved Resolution for 3-D Position Sensitive CdZnTe Spectrometers," *IEEE Trans. Nucl. Sci.*, vol. 51, No. 5, pp. 2427-2431, 2004.

[5] D. S. McGregor, Z. He, H. A. Seifert, D. K. Wehe, and R. A. Rojeski, "Single charge carrier type sensing with a parallel strip pseudo-Frisch- grid CdZnTe semiconductor radiation detector," *Appl. Phys. Lett.*, vol. 72, pp. 792-794, 1998.

[6] W. J. McNeil, D. S. McGregor, A. E. Bolotnikov, G. W. Wright, and R. B. James "Single-charge-carrier-type sensing with an insulated Frisch ring CdZnTe semiconductor radiation detector," *Appl. Phys. Lett.*, vol. 84, pp. 1988-1990, 2004.

[7] F. Zhang, C. Herman, Z. He, G. De Geronimo, E. Vernon, and J. Fried, "Characterization of the H3D ASIC readout system and 6.0 cm^3 3-D position sensitive CdZnTe detectors," *IEEE Trans. Nucl. Sci*., Vol. 59, No. 1, pp. 236-242, 2012.

[8] A. E. Bolotnikov, N. M. Abdul-Jabbar, S. Babalola, G. S. Camarda, Y. Cui, A. Hossain, E. Jackson, H. Jackson, J. R. James, A. L. Luryi, and R. B. James, "Optimization of virtual Frisch-Grid CdZnTe detector designs for imaging, and spectroscopy of gamma rays," *in Proc. SPIE*, Bellingham, WA, USA, 2007, vol. 6706, pp. 670603-1–670603-14, in Hard X-Ray and Gamma-Ray Detector Physics IX, 2005, SPIE.

[9] Y. Cui, A. Bolotnikov, G. Carmarda, A. Hossain, G. Yang, and R. B. James, "CZT virtual Frisch-grid detector: Principles and applications," in *Proc. 5th Annual IEEE Long Island Systems, Applications and Technology Conf.*, Farmingdale, NY, USA, 2009.

[10] J. K. Polack, M. Hirt, J. Sturgess, N. D. Sferrazza, A. E. Bolotnikov, S. Babalola, G. S. Carmarda, Y. Cui, S. U. Egarievwe, P. M. Fochuk, R. Gul, A. Hossain, K. Kim, O. V. Kopach, L. Marchini, G. Yang, L. Xu, and R. B. James, "Variation of electric shielding on virtual Frisch-Grid detectors," *Nucl. Instrum. Methods Phys. Res. A*, vol. 621, pp. 424–430, 2010.

[11] A. E. Bolotnikov, J. Butcher, G. S. Camarda, G. De Geronimo, J. Fried, R. Gul, P. M. Fochuk, M. Hamade, A. Hossain, K. H. Kim, O. V. Kopach, M. Petryk, E. Vernon, G. Yang, and R. B. James, "Array of virtual Frisch-Grid CZT detectors with common cathode readout for correcting charge signals and rejection of incomplete charge-collection events," *IEEE Trans. Nucl. Sci.*, vol. 59, no. 4, pp. 1544–1551, 2012.

[12] D. Herzo, R. Koga, W. A. Millard, S. Moon, J. Ryan, R. Wilson, A. D. Zych, and R. S. White "A large double scatter telescope for gamma rays and neutrons," *Nucl. Instrum. Methods Phys. Res. A*, vol. 251, pp. 132-134, 1974.

[13] M. Singh, "An electronically collimated gamma camera for single photon emission computed tomography. Part I: Theoretical considerations and design criteria," *Medical Physics*, vol. 10, pp. 421-427, 1983.

[14] Y. F. Du, Z. He, G. F. Knoll, D. K. Wehe, and W. Li, "Evaluation of Compton scattering camera using 3-D position sensitive CdZnTe detectors," *Nucl. Instrum.Methods Phys. Res. A*, vol. A457, pp. 203-211, 2001.

[15] C. E. Lehner, Z. He, and F. Zhang, "4π Compton imaging using a 3-D position-sensitive CdZnTe detector via weighted list-mode maximum likelihood," *IEEE Trans. Nucl. Sci.*, vol. 51, no. 4, pp. 1618-1624, 2004.

[16] W. Wang, C. Wahl, J. Jaworski, and Z. He, "Maximum-Likelihood Deconvolution in the Spatial and Spatial-Energy Domain for Events With Any number of iterations," *IEEE Trans. Nucl. Sci.*, vol. 59, no. 2, pp. 469-478, 2012.

[17] K. Vetter, M. Burks, C. Cork, M. Cunningham, D. Chivers, E. Hull, T. Krings, H. Manini, L. Michailescu, K. Nelson, D. Protic, J. Valentine, and D. Wright, "High sensitivity Compton imaging with position sensitive Si and Ge detectors," *Nucl. Instrum. Methods Phys. Res.* A, vol. A579, pp. 363-366, 2007.

[18] G. J. Schmid, D. A. Beckedahl, J. E. Kammeraad, J. J. Blair, K. Vetter, and A. Kuhn, "Gamma-ray Compton camera imaging with a segmented HPGe," *Nucl. Instrum. Methods Phys. Res. A*, vol. A459, pp. 565-576, 2001.

[19] A. P. Dempster, N. M. Laird, and D. B. Rubin, "Maximum likelihood from in complete data via the EM algorithm," *J. Royal Stat. Soc., Ser. B*, vol. 39, no. 1, pp. 1–38, 1977.

[20] K. Lange and R. Carson, "EM reconstruction algorithm for emission and transmission tomography," *J. Comput. Assist. Tomogr.*, vol. 8, no. 2, pp. 306–316, 1984.

[21] L. Parra and H. H. Barrett, "List-mode likelihood: EM algorithm and image quality estimation demonstrated on 2-D PET," *IEEE Trans. Med. Imag.*, vol. 17, no. 2, pp. 228–235, 1998.

[22] W. Lee, Ajin Jo, T. Lee, and D. Chu, "Monte Carlo Simulation on the 4π Field of a View Compact Compton Camera by Using Scintillators," *J. Kor. Phys. Soc.*, vol. 56, no. 1, pp. 20 – 27.Year?

[23] G. F. Knoll, *Radiation Detection and Measurement*, 3rd ed., New York, NY, Wiley, 2000, pp. 483.

[24] Y. F. Du, "Development of a Prototype Compton Scattering Camera Using 3-D Position Sensitive CZT Detectors," Ph.D. dissertation, Dept. Nuclear Engineering and Radiological Sciences, Univ. of Michigan, Ann Arbor, 2001.

[25] W. Lee, D. K. Wehe, M. Jeong, P. Barton, and J. Berry, "A dual modality gamma camera using $LaCl_3$(Ce) Scintillator," *IEEE Trans. Nucl. Sci*., vol. 56, no. 1, pp. 308–315, 2009.

[26] T. Lee and W. Lee "Portable Active Collimation Imager Using URA Patterned Scintillator," *IEEE Trans. Nucl. Sci*., vol. 61, no.14, pp. 654–662, 2014.